

## Metal Directed Assemblies of a Dipeptide: Formation of $\beta$ -Pleated Sheets

Nilotpal Barooah,<sup>[a]</sup> Rupam J. Sarma,<sup>[a]</sup> and Jubaraj B. Baruah\*<sup>[a]</sup>

**Keywords:** Hydrogen bonding / Self-assembly / Dipeptide /  $\beta$ -Sheets / Coordination polymer

The crystal structure of *N*-phthaloylglycylglycine and its complexes with copper(II) and zinc(II) are studied. The *N*-phthaloylglycylglycinato copper(II) complex has a polymeric structure formed by bridging carboxylates. The corresponding *N*-phthaloylglycylglycinato zinc(II) complex is mono-

meric. Both the metal complexes have self-assembled hydrogen-bonded structures in which dipeptide ligand adopt  $\beta$ -pleated conformations.

(© Wiley-VCH Verlag GmbH & Co. KGaA, 69451 Weinheim, Germany, 2006)

Directed assembly of molecules through noncovalent interactions and metal coordination is a fundamental process in nature.<sup>[1]</sup> Self-organization and molecular recognition of biomolecules<sup>[1c]</sup> using peptides are rationalized by taking into account a host of weak interactions<sup>[2]</sup> that include hydrogen bonding, aromatic  $\pi$  interactions, and hydrophobic interactions. The ability of peptides to adopt various secondary structures has been a subject of extensive study,<sup>[3]</sup> and in this regard the effects of metal ions in stabilizing particular conformations of peptides have immense importance.<sup>[4]</sup> The  $\beta$ -sheet assembly of peptide chains is particularly important in case of globular proteins and various template-directed strategies to assemble natural or non-natural peptides and synthetic peptide analogs into similar assemblies have been investigated.<sup>[5]</sup> Coordination of the peptide to a particular metal ion predominantly governs the local structure of the active site in metalloenzymes.<sup>[6]</sup> Even though attempts have been made to rationalize the interaction of metal ions with peptides,<sup>[7]</sup> the structural elucidation of such assemblies with regard to tuning the secondary interactions in the peptide<sup>[5b,8]</sup> is scarce. Given this background, we report the solid-state structures of the *N*-protected dipeptide derived from glycylglycine, and subsequently rationalize the effect of metal-ion templating on the self-assembly of this dipeptide.

Condensation of glycylglycine with phthalic anhydride under hydrothermal conditions and subsequent recrystallization from aqueous ethanol afforded the *N*-protected dipeptide, *N*-phthaloylglycylglycine (**L**) as colorless needles. The introduction of the phthaloyl group was expected to stabilize the two-dimensional assembly of the molecules in the solid state through intermolecular aromatic interactions.<sup>[9]</sup> These  $\pi$  interactions can be complementary in na-

ture to the intermolecular N–H $\cdots$ O interactions observed in case of amides, which have a dominating effect on the self-assembly process.<sup>[10]</sup> Crystal structure shows that the self-assembly of the dipeptide **L** in the solid state is governed by intermolecular hydrogen-bonding interactions; the molecule adopts a puckered conformation as shown in Figure 1. The amide N–H is involved in the formation of hydrogen bonds with the carbonyl oxygen atom of the phthalimide unit ( $d_{\text{N2}\cdots\text{O4}}$  3.04 Å;  $\angle$  D–H $\cdots$ A 156.0°), which extends along crystallographic *a* axis. Moreover, the amide carbonyl is strongly hydrogen-bonded to the oxygen atom of the carboxylic acid group ( $d_{\text{O1}\cdots\text{O3}}$  2.59 Å;  $\angle$  D–H $\cdots$ A 165.1°) as shown in Figure 1. Thus, intermolecular hydrogen-bonding interactions in **L** leads to the formation of two-dimensional sheets, wherein the individual molecules adopt folded conformations; however, the structure does not correspond to  $\beta$ -pleated sheet structure. The torsion angle for rotation about the C–N bond ( $\phi$ ) is 70.9° while the corresponding angle for the C–C bond rotation ( $\psi$ ) is 19.9°. The important hydrogen bond angles and bond lengths of **L** in the hydrogen-bonded assembly are listed in Table 1. It is important to note that the interplanar distance between the phthalimide groups of **L** is ca. 3.34 Å, which could indicate the presence of weak aromatic  $\pi$  interactions.

The templating effect of Cu<sup>II</sup> and Zn<sup>II</sup> ions, two of the biologically important metal ions, on the self-assembly of the dipeptide **L** has been studied by preparing the corresponding Cu<sub>2</sub>L<sub>4</sub>(H<sub>2</sub>O)<sub>4</sub>·2H<sub>2</sub>O and ZnL<sub>2</sub>(H<sub>2</sub>O)<sub>4</sub> complexes. Reaction of **L** with copper acetate mono hydrate results in the formation of the complex **1** which possess the molecular formula CuL<sub>2</sub>(H<sub>2</sub>O)<sub>2</sub>·2H<sub>2</sub>O. The crystal structure of **1** shows that each of the copper center is coordinated to **L** through the oxygen atoms of the carboxylate group; the coordinated water molecules are *trans* to each other in a nearly square-planar geometry with Cu1 $\cdots$ O1 and Cu1 $\cdots$ O6 bond lengths of 1.9471(10) and 1.9445(13) Å, respectively. The carbonyl oxygen of another adjacent glycinato unit leads to a weak Cu1 $\cdots$ O2 ( $d_{\text{Cu1}\cdots\text{O2}}$  2.650 Å) coordination,

[a] Department of Chemistry, Indian Institute of Technology, Guwahati, 781 039, India  
E-mail: juba@iitg.ernet.in

Supporting information for this article is available on the WWW under <http://www.eurjic.org> or from the author.

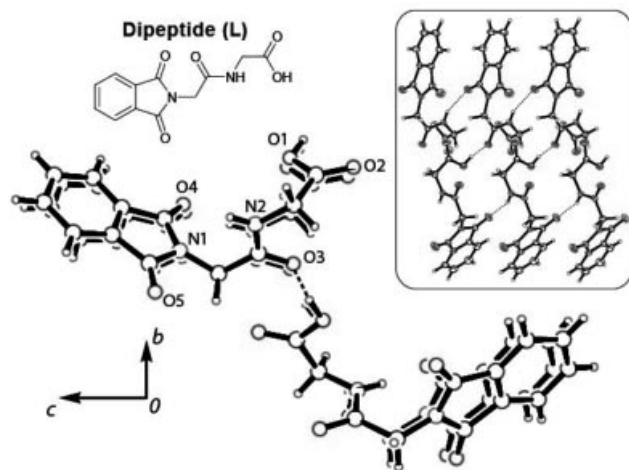


Figure 1. 2D Molecular sheets arising from intermolecular hydrogen bonding in **L**; (Inset) The hydrogen-bonded molecular sheets viewed parallel to *bc* plane.

Table 1. Hydrogen-bonding geometry (distances and angles) in *N*-phthaloylglycylglycine (**L**).

D–H...A	<i>d</i> <sub>D–H</sub> [Å]	<i>d</i> <sub>H...A</sub> [Å]	<i>d</i> <sub>D...A</sub> [Å]	∠ D–H...A [°]
N2–H...O4 <sup>#[a]</sup>	0.85	2.24	3.044	157.03
O1–H...O3 <sup>##</sup>	0.89	1.71	2.593	164.82

[a] Symmetry transformations used to generate atoms: <sup>#</sup> *x*–1, *y*, *z*, <sup>##</sup> *–x*+3/2, *y*+1/2, *–z*+1/2.

which gives the Cu<sup>II</sup> center axially distorted octahedral geometry as shown in Figure 2 (a). The unusual bridging mode of the carboxylate group in this coordination motif leads to a one-dimensional coordination network of Cu<sup>II</sup> ions along crystallographic *b* axis with Cu<sup>II</sup>...Cu<sup>II</sup> distance of 4.71 Å. The two O1...Cu1...O6 and O1...Cu1...O2 bond angles are 93.40° and 86.85°, respectively. The distorted octahedral geometry (Figure 2, b) of the Cu<sup>II</sup> center in complex **1** is also obvious from its ESR spectra. At room temperature, the ESR spectrum of the solid complex **1** shows a strong signal with center field at 3177.6 G (*g* = 2.124), which is an indication for the axially distorted octahedral geometry around the Cu<sup>II</sup> center. It may be pointed out

here that metal-directed self-assembled systems also give rise to porous metal-organic frameworks as well as coordination polymers.<sup>[11]</sup>

In the case of complex **1**, the water molecules included inside the lattice probably underlines the importance of water in stabilizing the  $\beta$ -sheets,<sup>[2]</sup> formed by the dipeptide units connected to the Cu<sup>II</sup> center. We have found that the ligand organization in this complex is governed by weak hydrogen-bonding interactions between the amide groups of the dipeptide and the interstitial water molecules. In this complex, intermolecular hydrogen bonding between the amide N–H groups and the amide carbonyl groups (*d*<sub>N1...O3</sub> 2.94 Å; ∠ D–H...A 157.8°) is complemented by weak C–H...O interaction involving C4–H as donor and O3 as acceptor (*d*<sub>C4...O3</sub> 3.05 Å). This weak C–H...O interaction is well within the range reported elsewhere.<sup>[2b]</sup> These two weak interactions assemble the *N*-phthaloylglycylglycinato ligands leading to a parallel  $\beta$ -pleated sheet conformation as shown in the Figure 2 (a). The torsion angle for rotation about the C–N bond ( $\varphi$ ) is –135.3°, while the corresponding angle for the C–C bond rotation ( $\psi$ ) is 169.2° which is within the limit of  $\beta$ -sheet structure.<sup>[3a–3b]</sup> This corresponds to a *trans* conformation about the C–C bond.<sup>[3b]</sup> The hydrogen-bond donor...acceptor distances and angles of complex **1** are listed in Table 2.

Table 2. Hydrogen bonding geometry (distances and angles) in complex **1**<sup>[a]</sup>.

D–H...A	<i>d</i> <sub>D–H</sub> [Å]	<i>d</i> <sub>H...A</sub> [Å]	<i>d</i> <sub>D...A</sub> [Å]	∠ D–H...A [°]
N1–H...O3 <sup>#[b]</sup>	0.79	2.18	2.944	162.3
O6–H...O7 <sup>##</sup>	0.81	1.89	2.668	158.5
O6–H...O2	0.81	1.88	2.650	157.7
O7–H...O2+ <sup>###</sup>	0.74	2.11	2.851	170.5

[a] O6 is from coordinated water; O7 is from interstitial water.

[b] Symmetry transformations used to generate atoms: <sup>#</sup> *x*, *y*+1, *z*; <sup>##</sup> *x*–1, *y*+1, *z*+1, <sup>###</sup> *–x*+1, *y*, *–z*+3/2.

In a similar way, the Zn<sup>II</sup> complex ZnL<sub>2</sub>(H<sub>2</sub>O)<sub>4</sub> (**2**) was synthesized and structurally characterized. Each Zn<sup>II</sup> ion is coordinated to two monodentate carboxylic groups of **L** and four water molecules; which results in an octahedral

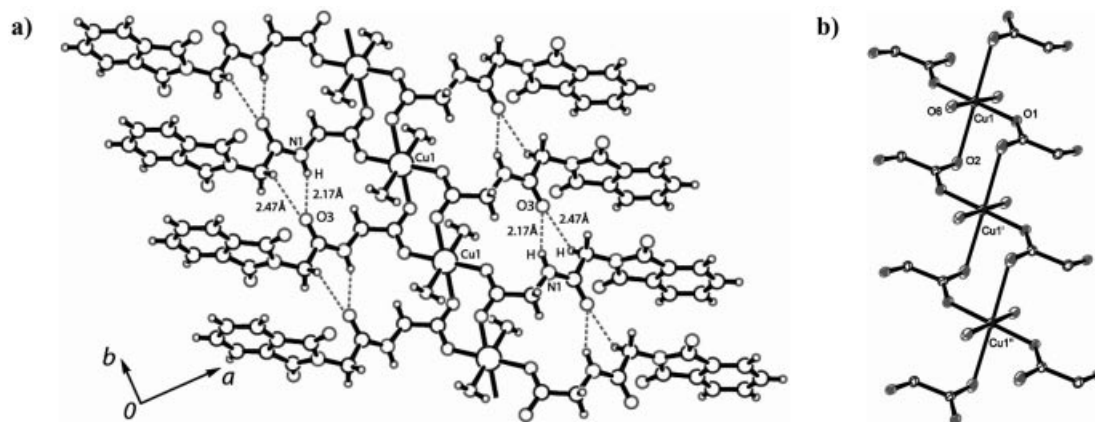


Figure 2. (a) Structure of the hydrogen-bonded sheets in complex **1** (interstitial water molecules are excluded for clarity); (b) Coordination environment of Cu<sup>II</sup> centers in the complex (thermal ellipsoids drawn to 30% probability).

coordination environment around each  $\text{Zn}^{\text{II}}$  center as shown in Figure 3. The  $\text{Zn1}\cdots\text{O1}$ ,  $\text{Zn1}\cdots\text{O6}$  and  $\text{Zn1}\cdots\text{O7}$  bond lengths are 2.0921(15), 2.0586(16), 2.1429(16) Å, respectively. The crystal structure of **2** also reveals that the *N*-phthaloyl-protected dipeptide residues assemble through intermolecular  $\text{N1-H}\cdots\text{O3}$  hydrogen bonds ( $d_{\text{N1}\cdots\text{O3}}$  3.04 Å;  $\angle \text{D-H}\cdots\text{A}$  157.8°) along with weak  $\text{C4-H}\cdots\text{O3}$  interactions ( $d_{\text{C4}\cdots\text{O3}}$  3.11 Å). These two weak interactions lead to the formation of parallel  $\beta$ -pleated sheets as shown in Figure 3.

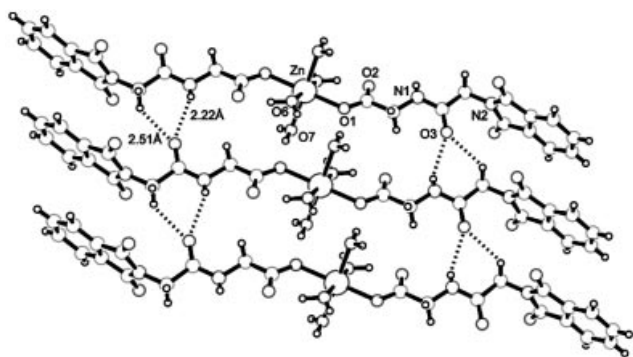


Figure 3. Ligand organization around the  $\text{Zn}^{\text{II}}$  centers of the complex **2**.

It is noteworthy that in both the structures of complexes **1** and **2**, the presence of coordinated water as well as the interstitial water molecules (in case of **1**) is crucial in stabilizing the self-assembled  $\beta$ -pleated sheets. The hydrogen bond lengths and bond angles that are involved in the formation in complex **2** are listed in Table 3. The torsion angle for rotation about the C–N bond ( $\varphi$ ) in this case is  $-153.6^\circ$  and for the C–C bond rotation ( $\psi$ ) is  $165.7^\circ$ , which are similar to those in the complex **1** and is indicative of  $\beta$ -pleated sheets.<sup>[2b]</sup>

Table 3. Hydrogen bonding geometry (distances and angles) in complex **2**.

D–H $\cdots$ A	$d_{\text{D-H}}$ [Å]	$d_{\text{H}\cdots\text{A}}$ [Å]	$d_{\text{D}\cdots\text{A}}$ [Å]	$\angle \text{D-H}\cdots\text{A}$ [°]
N1–H $\cdots$ O3 [x, y + 1, z]	0.86	2.23	3.044	157.8
O6–H $\cdots$ O2	1.03	1.65	2.652	159.7
O7–H $\cdots$ O1 [x, y + 1, z]	0.80	1.88	2.672	170.4

The presence of two interstitial water molecules per formula unit in complex **1** has a structural role to play, as they hold the hydrogen-bonded dipeptide  $\beta$ -sheets (Figure 4, a) through intermolecular  $\text{O7-H}\cdots\text{O2}$  ( $d_{\text{O7}\cdots\text{O2}}$  2.85 Å;  $\angle \text{D-H}\cdots\text{A}$  170.5°) and  $\text{O7-H}\cdots\text{O5}$  ( $d_{\text{O7}\cdots\text{O5}}$  2.99 Å;  $\angle \text{D-H}\cdots\text{A}$  165.7°) interactions. Furthermore, each interstitial water molecule is bound to a coordinated water molecule through intermolecular  $\text{O6-H}\cdots\text{O7}$  ( $d_{\text{O6}\cdots\text{O7}}$  2.66 Å;  $\angle \text{D-H}\cdots\text{A}$  158.5°) hydrogen bonds. The presence two interstitial water molecules in the lattice is reflected in the thermogram of the compound, which shows 8.9% weight loss in the temperature range 75–120 °C corresponding to loss of three water molecules (theoretical weight loss 8.2%) corresponding to interstitial and coordinated water molecules. In the case of **2**, the coordinated water molecules are involved in intramolecular  $\text{O6-H}\cdots\text{O7}$  ( $d_{\text{O6}\cdots\text{O7}}$  2.91 Å;  $\angle \text{D-H}\cdots\text{A}$  149.9°) and intermolecular  $\text{O7-H}\cdots\text{O4}$  ( $d_{\text{O7}\cdots\text{O4}}$  3.02 Å;  $\angle \text{D-H}\cdots\text{A}$  150.2°) hydrogen-bonding interactions. These interactions stabilize the formation of individual  $\beta$ -pleated sheets in **1** and **2** as shown in Figure 4, parts a and b, respectively. Thermogravimetric analysis of complex **2** (please refer to supporting information, for supporting information see also the footnote on the first page of this article) shows that the four-coordinated water molecules are lost between 70–135 °C, which corresponding to about 9.3% weight loss (theoretically calculated weight loss for such process corresponds to 10.9%).

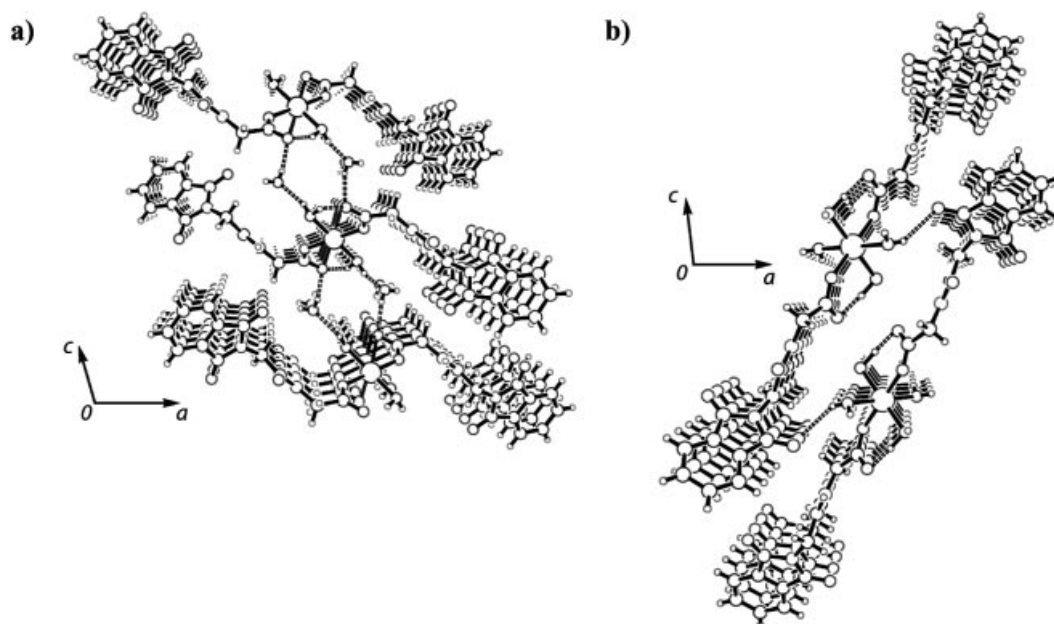


Figure 4. (a) Packing pattern of **1** (viewed along *b* axis); (b) packing pattern of **2** (viewed along *b* axis).



Thus, we have structurally characterized the solid-state assemblies of *N*-phthaloylglycylglycine that are formed through intermolecular hydrogen bonding, and shown that the self-assembly of this molecule can be tuned to adopt a  $\beta$ -sheet conformation by introduction of metal ions, in this case  $\text{Cu}^{\text{II}}$  and  $\text{Zn}^{\text{II}}$ . It is found that the parallel  $\beta$ -pleated sheet assembly of the dipeptide leads to a one-dimensional  $\text{Cu}^{\text{II}}$  carboxylate coordination polymer through carboxylate bridging in a different manner over conventional paddle-wheel-type of structures.<sup>[12]</sup> Currently, we are studying the different motifs that are crucial in the metal template assembly of similar dipeptides and higher analogs.

## Experimental Section

The X-ray diffraction data were collected at room temperature with a Bruker 3-circle diffractometer (Bruker Nonius SMART APEX 2) equipped with CCD area detectors, and using graphite-monochromated  $\text{Mo-K}_\alpha$  radiation ( $\lambda = 0.71073 \text{ \AA}$ ) from 60W microfocus Siemens Microsource with glass polycapillary optics. X-ray diffraction data for all the crystals were collected with Bruker SMART software. This software was also used for indexing and determining the unit cell parameters. The structures were solved by direct methods and refined by full-matrix least-squares against  $F^2$  for all data using SHELXTL software.<sup>[14]</sup> All non-H atoms were refined by full-matrix least-squares in the anisotropic approximation and the hydrogen atoms attached to these atoms were treated as “riding” in calculated positions in the case of complex **2**; with **L** and complex **1** the hydrogen atoms were located on the difference Fourier maps. In all cases, the hydrogen atoms attached to polar atoms such as O and N were located on the difference Fourier maps and refined in the final structure in isotropic approximation.

CCDC-297186 (for **1**), -297187 (for **2**) and -299730 (for **L**) contain the supplementary crystallographic data for this paper. These data can be obtained free of charge from The Cambridge Crystallographic Data Centre via [www.ccdc.cam.ac.uk/data\\_request/cif](http://www.ccdc.cam.ac.uk/data_request/cif).

Glycylglycine, phthalic anhydride, copper(II) acetate dihydrate and zinc(II) acetate dihydrate were procured from Fluka and used as received. The NMR spectra were recorded with a Varian 400 MHz spectrophotometer at room temperature while the FT-IR spectra were recorded with Nicolet Impact-410 spectrometer using OMNIC software.

**Synthesis of *N*-Phthaloylglycylglycine (**L**):** A finely ground mixture of phthalic anhydride (0.444 g, 3 mmol) and glycylglycine (0.396 g, 3 mmol) was heated to approximately 175 °C in a 50-mL round-bottomed flask. The molten mixture was cooled to room temperature, and the resulting solid was purified by recrystallization from ethanol/water (1:9, v/v) mixture to obtain the product. Yield: 0.30 g (39%). IR (KBr):  $\tilde{\nu} = 3363$  (s), 2935 (br. s), 2873 (br. s), 2597 (s), 1737 (s), 1701 (s), 1621 (s), 1543 (s), 1419 (s), 1393 (s), 1332 (w), 1230 (s), 1107 (w), 953 (s), 728 (w)  $\text{cm}^{-1}$ .  $^1\text{H}$  NMR ( $[\text{D}_6]\text{DMSO}$ ):  $\delta = 12.8$  (br. s, 1  $\text{H}_{\text{COOH}}$ ), 8.5 (s, 1  $\text{H}_{\text{NH}}$ ), 7.8 (m, 4 H), 4.2 (s, 2 H), 3.7 (d,  $J = 5.6 \text{ Hz}$ , 2 H) ppm.  $^{13}\text{C}$  NMR ( $[\text{D}_6]\text{DMSO}$ ):  $\delta = 176.1, 172.7, 171.7, 139.9, 137.1, 128.5, 46.2, 45.7$  ppm.

**Synthesis of Complex 1:** A solution of copper(II) acetate dihydrate (0.100 g, 0.5 mmol) in ethanol (20 mL) was added dropwise to a homogeneous stirred solution of **L** (0.263 g, 1 mmol) in ethanol/water (20 mL, 1:9, v/v) at room temperature. Light blue precipitate had started appearing within 15 minutes of addition of the ligand. The solution was stirred for another two hours, and the resulting

precipitate was filtered and washed with ethanol. The precipitate was redissolved in 20 mL of distilled water, concentrated to 10 mL, and left undisturbed. After three days light blue needle-like crystals of the product were collected by filtration and dried in air. Yield for the crystalline product: 0.067 g (20% based on Cu). IR (KBr):  $\tilde{\nu} = 3590$  (s), 3309 (s), 3094 (br. s), 1772 (w), 1726 (s), 1658 (s), 1562 (s), 1409 (s), 1322 (w), 1265 (w), 1122 (w), 958 (s), 758 (s), 723 (s)  $\text{cm}^{-1}$ .

**Synthesis of Complex 2:** A solution of zinc(II) acetate dihydrate (0.110 g, 0.5 mmol) in 20 mL ethanol was added dropwise to a homogeneous stirred solution of **L** (0.263 g, 1 mmol) in ethanol/water (20 mL, 1:1, v/v) at room temperature. Off-white precipitate had started appearing within 15 minutes of addition. The solution was stirred for another two hours, and the resulting precipitate was filtered and washed with ethanol. The precipitate was redissolved in 20 mL of distilled water, concentrated to 10 mL and left undisturbed. After five days light colorless plate-like crystals of the product were collected by filtration and dried in air. Yield for the crystalline product: 0.078 g (23% based on Zn). IR (KBr):  $\tilde{\nu} = 3534$  (s), 3319 (s), 3075 (br. s), 1770 (w), 1722 (s), 1650 (s), 1551 (s), 1411 (s), 1311 (w), 1246 (w), 1116 (w), 955 (s), 755 (s), 715 (s)  $\text{cm}^{-1}$ .  $^1\text{H}$  NMR ( $[\text{D}_6]\text{DMSO}$ ):  $\delta = 8.3$  (s, 1  $\text{H}_{\text{NH}}$ ), 7.8 (m, 4 H), 4.2 (s, 2 H), 3.6 (d,  $J = 4.4 \text{ Hz}$ , 2 H) ppm.

**Supporting Information** (see also the footnote on the first page of this article) is available for selected crystallographic data, FT-IR spectra of the dipeptide and complex **1**, the ESR spectrum of **1** and  $^1\text{H}$  HOMOCOSY spectra of complex **2**.

## Acknowledgments

The authors thank DST (India) for financial support.

- [1] a) J. M. Lehn, *Science* **2002**, 295, 2400–2403; b) G. M. Whitesides, B. Grzybowski, *Science* **2002**, 295, 2418–2421; c) C. Piguet, G. Bernardinelli, G. Hopfgartner, *Chem. Rev.* **1997**, 97, 2005–2062; d) A. Nurit, W. S. Horne, R. M. Ghadiri, *Small* **2006**, 2, 99–102; e) S. M. Butterfield, M. L. Waters, *J. Am. Chem. Soc.* **2003**, 125, 9580–9581.
- [2] a) E. A. Meyer, R. K. Castellano, F. Diederich, *Angew. Chem. Int. Ed.* **2003**, 42, 1210–1250; b) G. R. Desiraju, T. Steiner, *The Weak Hydrogen Bonds in Structural Chemistry and Biology*, Oxford University Press, **1999**, Oxford; c) T. Steiner, *Angew. Chem. Int. Ed.* **2002**, 41, 48–76.
- [3] a) D. Seebach, D. F. Hook, A. Glattli, *Biopolymers* **2006**, 84, 23–37; b) R. P. Cheng, S. H. Gellman, W. F. DeGrado, *Chem. Rev.* **2001**, 101, 3219–3232; c) J. T. Pelton, L. R. McLean, *Anal. Biochem.* **2000**, 277, 167–176.
- [4] a) D. L. Minor Jr, P. S. Kim, *Nature* **1994**, 367, 360–363; b) C. A. Kim, J. M. Berg, *Nature* **1993**, 362, 267–270; c) D. L. Minor Jr, P. S. Kim, *Nature* **1994**, 371, 264–267; d) L. Regan, W. F. DeGrado, *Science* **1988**, 241, 976–978; e) Z.-Q. Tian, P. A. Bartlett, *J. Am. Chem. Soc.* **1996**, 118, 943–949; f) A. Pessi, E. Bianchi, A. Crameri, S. Venturini, A. Tramontano, M. Sollazzo, *Nature* **1993**, 362, 367–369.
- [5] a) M. D. Struthers, R. P. Cheng, B. Imperiali, *J. Am. Chem. Soc.* **1996**, 118, 3073–3081; b) J. P. Snyder, A. S. Lakdawala, M. J. Kelso, *J. Am. Chem. Soc.* **2003**, 125, 632–633; c) E. L. Baker, R. E. Hubbard, *Prog. Biophys. Mol. Biol.* **1984**, 44, 97–179; d) V. Venkatraman, S. V. Shankaramma, P. Balaram, *Chem. Rev.* **2001**, 101, 3131–3152; e) J. S. Nowick, S. Mahrus, E. M. Smith, J. W. Ziller, *J. Am. Chem. Soc.* **1996**, 118, 1066–1072; f) J. F. Espinosa, S. H. Gellman, *Angew. Chem. Int. Ed.* **2000**, 39, 2330–2333.

- [6] a) S. J. Lippard, J. M. Berg, *Principles of Bioinorganic Chemistry*, University Science Books, **1994**; b) J. J. R. Frausto Da Silva, R. J. P. Williams, *The Biological Chemistry of The Elements: The Inorganic Chemistry of Life*, Oxford University Press, Oxford, **2001**; c) M. A. Halcrow, *Angew. Chem. Int. Ed.* **2001**, *40*, 346–349.
- [7] a) K. Suzuki, H. Hiroaki, D. Kohda, H. Nakamura, T. Tanaka, *J. Am. Chem. Soc.* **1998**, *120*, 13008–13015; b) M. R. Ghadiri, C. Soares, C. Choi, *J. Am. Chem. Soc.* **1992**, *114*, 4000–4002; c) M. R. Ghadiri, C. Soares, C. Choi, *J. Am. Chem. Soc.* **1992**, *114*, 825–831; d) W. S. Horne, D. C. Stout, M. R. Ghadiri, *J. Am. Chem. Soc.* **2003**, *125*, 9372–9376; e) D. T. Bong, M. R. Ghadiri, *Angew. Chem. Int. Ed.* **2001**, *40*, 2163–2166; f) M. R. Ghadiri, C. Choi, *J. Am. Chem. Soc.* **1990**, *112*, 1630–1632.
- [8] a) K. Haas, W. Ponikwar, H. Nöth, W. Beck, *Angew. Chem. Int. Ed.* **1998**, *37*, 1086–1089; b) C. S. Burns, E. Aronoff-Spencer, C. M. Dunham, P. Lario, N. I. Avdievich, W. E. Antholine, M. M. Olmstead, A. Vrielink, G. J. Gerfen, J. Peisach, W. G. Scott, G. L. Millhauser, *Biochemistry* **2002**, *41*, 3991–4001.
- [9] a) N. Barooah, R. J. Sarma, A. S. Batsanov, J. B. Baruah, *Polyhedron* **2006**, *25*, 17–24; b) N. Barooah, R. J. Sarma, J. B. Baruah, *Cryst. Growth Des.* **2003**, *3*, 639–641.
- [10] R. J. Sarma, J. B. Baruah, *CrystEngComm* **2005**, *7*, 706–771; M. A. Halcrow, *Dalton Trans.* **2003**, 23, 4375–4384.
- [11] a) O. M. Yaghi, M. O’Keeffe, N. W. Ockwig, H. K. Chae, M. Eddaoudi, J. Kim, *Nature* **2003**, *423*, 705–714; b) O. M. Yaghi, H. Li, C. Davis, D. Richardson, T. L. Groy, *Acc. Chem. Res.* **1998**, *31*, 474–484; c) H. Y. An, E.-B. Wang, D. R. Xiao, Y. G. Li, Z. M. Su, L. Xu, *Angew. Chem. Int. Ed.* **2006**, *45*, 904–908; d) X.-J. Luan, Y.-Y. Wang, D.-S. Li, P. Lie, H.-M. Hu, Q.-Z. Shi, S.-M. Peng, *Angew. Chem. Int. Ed.* **2005**, *44*, 3864–3867; e) F. M. Tabellion, S. R. Seidel, A. M. Arif, P. J. Stang, *Angew. Chem. Int. Ed.* **2001**, *40*, 1529–1532; f) R. Matsuda, R. Kitaura, S. Kitagawa, Y. Kubota, T. C. Kobayashi, S. Horika, M. Takata, *J. Am. Chem. Soc.* **2004**, *126*, 14063–14070; g) J. V. Barth, G. Costantini, K. Kern, *Nature* **2005**, *437*, 671–679.
- [12] a) G. M. Brown, M. George, R. Chidambaram, *Acta Crystallogr., Sect. B* **1973**, *29*, 2393–2403; b) K. Seki, *Chem. Commun.* **2001**, 1496–1497.
- [13] a) G. M. Sheldrick, *SHELXS97, Program for the solution of crystal structures*, Univ. of Göttingen, Germany, **1997**; b) G. M. Sheldrick, *SHELXS97, Program for the refinement of crystal structures*, Univ. of Göttingen, Germany, **1997**.
- [14] G. M. Sheldrick, *SHELXTL, The complete software package for single crystal structure determination*, release 5.10, Bruker AXS, Inc., Madison, **1997**.

Received: March 10, 2006

Published Online: June 14, 2006